Proceedings of Nuclear and Emerging Technologies for Space 2011
Albuquerque, NM, February 7-10, 2011
Paper 3335

Evaluating Heat Pipe Performance in 1/6 g Acceleration: Problems and Prospects

Donald A. Jaworske[1a], Timothy A. McCollum[2], Marc A. Gibson[1b], James L. Sanzi[3], and Edward A. Sechkar[4]

[1a]Space Environment and Experiments Branch and [1b]Thermal Energy Conversion Branch, NASA Glenn Research Center, Cleveland, OH 44135
[2]Mathematics and Science Division, Hagerstown Community College, Hagerstown, MD 21742
[3]Sest, Inc., Middleburg Heights, OH 44130
[4]ASRC Aerospace Corp., NASA Glenn Research Center, Cleveland, OH 44135
(216) 433-2312; Donald.A.Jaworske@nasa.gov

Abstract. Heat pipes composed of titanium and water are being considered for use in the heat rejection system of a fission power system option for lunar exploration. Placed vertically on the lunar surface, the heat pipes would operate as thermosyphons in the 1/6 g environment. The design of thermosyphons for such an application is determined, in part, by the flooding limit. Flooding is composed of two components, the thickness of the fluid film on the walls of the thermosyphon and the interaction of the fluid flow with the concurrent vapor counter flow. Both the fluid thickness contribution and interfacial shear contribution are inversely proportional to gravity. Hence, evaluating the performance of a thermosyphon in a 1 g environment on Earth may inadvertently lead to overestimating the performance of the same thermosyphon as experienced in the 1/6 g environment on the moon. Several concepts of varying complexity have been proposed for evaluating thermosyphon performance in reduced gravity, ranging from tilting the thermosyphons on Earth based on a cosine function, to flying heat pipes on a low-g aircraft. This paper summarizes the problems and prospects for evaluating thermosyphon performance in 1/6 g.

Keywords: Heat Pipe, Thermosyphon.

INTRODUCTION

Fission power systems utilized on the moon or Mars will require radiators equipped with heat pipes to provide cooling. Heat pipes divide the radiator into many segments, with each segment dissipating heat from a heat pipe in order to provide a means to mitigate the risk of micrometeoroid impact. Placed vertically, the heat pipes operate as thermosyphons where gravity plays a role in heat pipe operation. In the closed two-phase thermosyphon system, energy is absorbed through the wall of the evaporator. The working fluid contained in the evaporator undergoes a phase change and vapor moves through the center of the pipe to the condenser. A second phase change occurs at the condenser wall. Energy is released to the surroundings, and working fluid returns to the evaporator as a fluid film on the interior surface of the pipe. This process requires little temperature difference between evaporator and condenser. For a thermosyphon, fluid return to the evaporator relies on gravity. Indeed, a thermosyphon cannot work against gravity. Much work has been done to study the performance characteristics and working dynamic of closed two-phase thermosyphons on Earth at 1g. However, very little work has been done to study the performance characteristics and limitations of thermosyphons in a reduced gravity environment. Because of the plan to include titanium-water thermosyphons in fission power systems for use on the moon or Mars, it is important to begin to generate data and gather firsthand knowledge of how the performance of such closed two-phase thermosyphons may be affected by a reduced gravity environment.

PROBLEMS

There are several concepts for evaluating thermosyphon performance in a reduced gravity environment. The simplest technique is to tilt the thermosyphon. The angle of tilt is selected utilizing the cosine function, such that the gravity vector in the axial direction of the thermosyphon is reduced by the desired amount. An angle of 9.5° simulates the lunar surface. This geometric approach offers the advantage of simplicity. Tilting a thermosyphon to 9.5° above horizontal to simulate 1/6 g was utilized successfully during the Second Generation Radiator Demonstration Unit evaluation conducted at Glenn Research Center in 2009 (Ellis, 2010). In short, tilting the panel had little effect on the performance of the Second Generation Radiator Demonstration Unit thermosyphons and the radiator panel thermal performance.

The problem with tilting a thermosyphon is that the dynamics of fluid flow and vapor flow inside the pipe are changed. For a case incorporating uniform heat transfer to the surroundings, the fluid film generated in a vertical thermosyphon is uniformly distributed around the interior surface of the condenser and vapor flow is axisymmetric. However, the process of tilting introduces uncertainties in the distribution of liquid along the wall interior which may impact heat transfer through the working fluid. The fluid film generated in a tilted thermosyphon is under the influence of gravity which creates a dearth of fluid on the ceiling of the interior surface, an excess of fluid on the bottom of the interior surface, and vapor flow is no longer axisymmetric.

Another avenue for evaluating thermosyphon performance in a reduced gravity environment is through the use of a drop tower. In an evacuated drop tower, microgravity conditions prevail with durations on the order of a few seconds. The problem with utilizing a drop tower is that 1/6 g would have to be superimposed on the microgravity environment by utilizing a mechanical structure such as a centrifuge. The acceleration field over the length of any reasonably sized thermosyphon in a centrifuge would be non-uniform, and the size and rotation rate of the centrifuge would be prohibitive.

One concept which appears promising for evaluating the performance of a thermosyphon in a reduced gravity environment is through the use of low-g aircraft flights. In an aircraft flying a specific parabolic pattern, microgravity conditions with durations on the order of tens of seconds can be obtained. Flying slightly different parabolic flight paths can create 1/6 g and 1/3 g environments for comparable times. Such a duration of 1/6 g could be utilized to generate data and gather firsthand knowledge on thermosyphon operation, given a suitably constructed test rig.

PROSPECTS

If a process prevents a thermosyphon from operating at equilibrium, the maximum effective thermal conductivity of the thermosyphon is limited. Some of the processes that limit heat transfer in a thermosyphon are, the sonic limit, the condenser limit, the entrainment limit, and the flooding limit.

The sonic limit is derived from a limitation imparted by the compressible nature of the working vapor, and occurs at very low vapor densities and very high vapor velocities. At the onset of the sonic limit vapor flow is choked at the exit of the evaporator. In practice the sonic limit is a consideration only during start up or when the thermosyphon is designed to have a very narrow cross sectional area.

The condenser limit occurs due to a cooling limitation of the condenser. An insufficient ability to transfer energy from the condenser to the environment, because of an inadequate coupling to the environment by conduction, convection, or radiation brought about by a poor heat sink or fin assembly can limit the heat transport capability by slowing the condensation rate of the vapor onto the condenser wall.

The flooding limit is attributed to the interfacial sheer force at the boundary between the liquid and vapor, is characterized by high vapor velocities, and occurs when the concurrent vapor flow is so severe that the liquid flow is prevented from reaching the evaporator and floods the condenser. The entrainment limit is also attributed to the interfacial sheer force at the boundary between the liquid and vapor, and is the result of drops of liquid that are captured by the vapor flow and carried back to the condenser, creating an insufficient liquid volume in the evaporator. Note that the entrainment limit is characterized by liquid droplets in the vapor while the flooding limit is driven by viscous and surface tension forces alone (Faghri, 1995). Flooding results in a rapid temperature rise of

the evaporator, and a severe decrease in the effective thermal conductivity of the thermosyphon. The onset of the flooding limit corresponds to the maximum heat transport rate of a given thermosyphon. The flooding limit is illustrated in Figure 1.

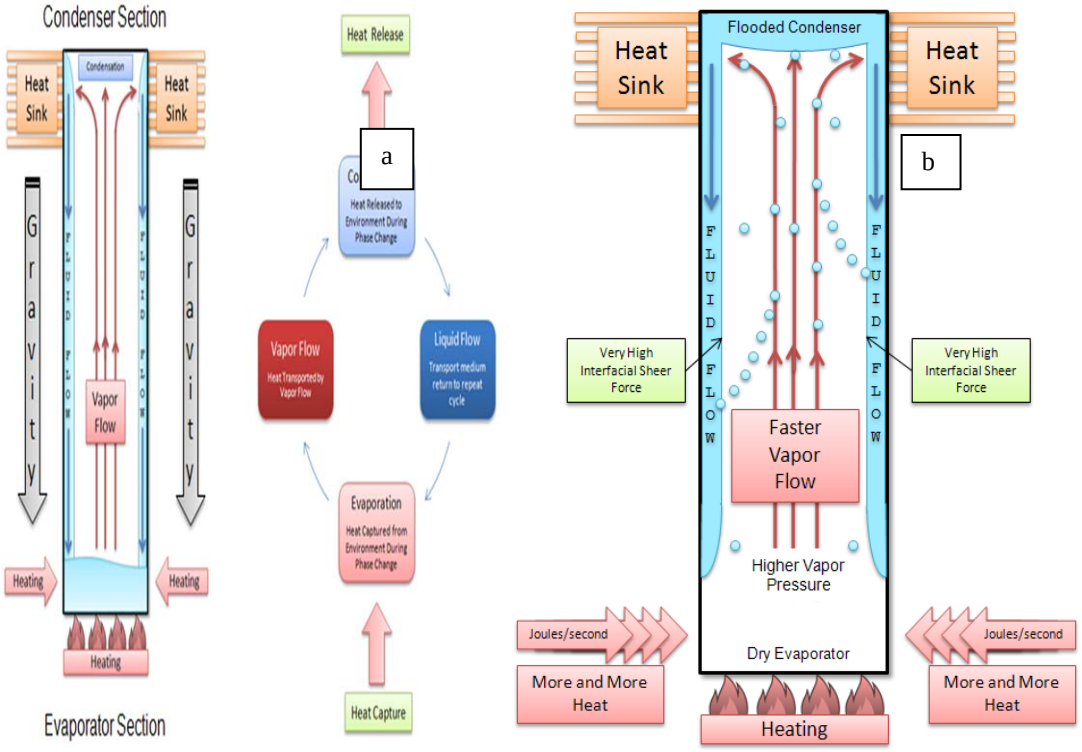

FIGURE 1. Closed Two-Phase Thermosyphon, a) Under Normal Operation and b) at the Onset of Flooding and Entrainment.

The amount of energy removed from the environment per unit time (Q) by a thermosyphon is a function of the heat of vaporization (h_g) of the working fluid and the mass flow rate ($\dot{m}$) of the working fluid, and is given by Equation 1.

$$Q = \dot{m}\, h_g \tag{1}$$

At steady state, the mass flow of vapor from evaporator to condenser equals mass flow of liquid from condenser to evaporator. For a known input power, this equilibrium mass flow can be calculated by rearranging Equation 1.

$$\dot{m} = \frac{Q}{h_g} \tag{2}$$

Shatto et al. (1996) give an analytic model for the fluid flowing down the wall of a thermosyphon as a function of equilibrium mass flow, $\dot{m}$, in a thermosyphon, based on the work of Katto and Watanabe (1992). If Equation 2 is used for $\dot{m}$, Equation 3 gives a relation for the thickness of the fluid film as a function of input power, Q.

$$\frac{\delta}{R} = \frac{3}{2}\left(\frac{\dot{m}\mu_L}{\pi\rho_L{}^2 g\delta^2 R^2} + \frac{\tau_i}{\rho_L g R}\right) \tag{3}$$

Equation 3 can be used to determine the flooding limit. The first term in Equation 3 includes mass flow, viscosity of the liquid (μ_L), density of the liquid (ρ_L), acceleration due to gravity (g), fluid film thickness (δ), and pipe radius (R), and represents the effect of the condensing vapor on the fluid film thickness similar to a Nusselt analysis of a

laminar flow on a vertical flat plate. In the first term, the dependence on gravity appears as the reciprocal of the acceleration due to gravity. The second term in Equation 3 includes the interfacial shear force between the fluid and the vapor (τ_i), density of the liquid density, the acceleration due to gravity, and pipe radius, and represents the interaction of the fluid flow with the concurrent vapor flow. The term τ_i is given by Equations 4, 5 and 6, where C_{fi} is an empirically determined dimensionless constant, σ is surface tension, and B_o is the Bond number.

$$\tau_i = \frac{\rho_v}{2}\left[\left(1 - \frac{\rho_v R}{\rho_L 2\delta}\right)\frac{\dot{m}}{\rho_v \pi R^2}\right]^2 C_{fi} \tag{4}$$

$$C_{fi} = \left[0.005 + 0.2574\left(\frac{\delta B_o}{2R}\right)^{1.63+\frac{4.74}{B_o}}\right] 10^{\frac{9.07}{B_o}} \tag{5}$$

$$B_o = D\sqrt{\frac{g(\rho_L - \rho_v)}{\sigma}} \tag{6}$$

The interfacial sheer force depends on gravity in a much more complex way being brought into the analysis through the Bond number. To determine the flooding limit one must determine from Equation 2 what value of $\dot{m}$, or equivalently Q, separates the regions where $\delta(Q)$ has and does not have solutions. Equation 3 is a transcendental equation. No closed solution exists for $\delta(Q)$ and this equation must be solved numerically or graphically.

Figure 2 shows an example of a graphical solution to this equation for a water thermosyphon with an inner tube radius of 4.57 mm under Earth gravity. It should be noted that for this graph average values were used for the physical properties of water and that temperature dependence of these properties were not included in the analysis. In Figure 2, the family of curves shown is the right hand side of Equation 3 plotted as a function of the dimensionless variable δ/R for different values of Q. Equation 2 was used to calculate $\dot{m}$ for each Q. The 45° line shown in the graph is simply the equality $\delta/R = \delta/R$. A curve corresponding to a given input power Q can either intersect the 45° line one time, two times, or not at all. If the curve intersects the 45° line once, the solution for the fluid film thickness δ for that particular input power Q is given by the value of δ/R where the intersection occurs. If the curve intersects the 45° line twice the value that corresponds to the physically observable fluid film thickness is given by the intersection occurring at the smaller value of δ/R. If a curve does not intersect the 45° line at all, it means that there is no solution to Equation 3 for this value of Q. The case of no solution physically means that the thermosyphon cannot function in equilibrium for this value of Q and that the flooding limit of the thermosyphon has been surpassed. Five different input powers are shown in Figure 2. The first three curves, 200 W, 300 W, and 400 W, all intersect the 45° line twice, so the thermosyphon can operate at equilibrium at these power levels. The fourth curve, 475 W, intersects the 45° line once. The thermosyphon can still operate in equilibrium at this power level, but any further increase in the input power will result in a curve that does not intersect the 45° line, as shown by the 575 W curve. As a result, one can conclude that the boundary between equilibrium operation of this thermosyphon and the onset of the flooding limit should occur at an input power of approximately 475 W.

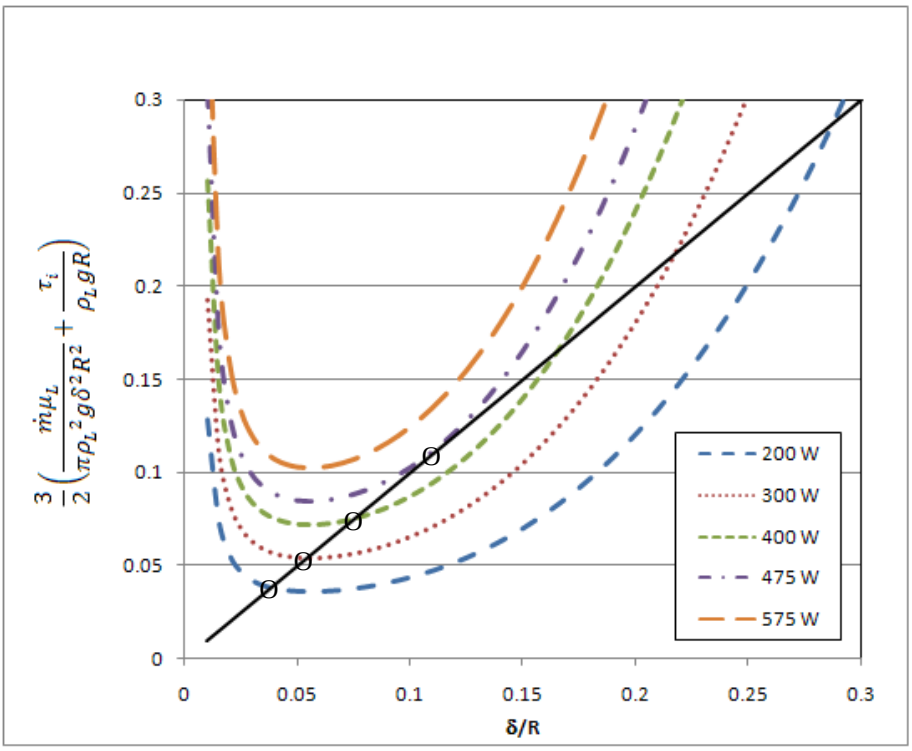

FIGURE 2. Graphical Solution to Equation 3 using Average Physical Properties of Water for a 4.57 mm Radius Thermosyphon.

This treatment was utilized to design a test rig for flight on a low-g aircraft. The test rig consists of three basic components. First, the test rig contains a thermosyphon array containing twelve identical thermosyphons. Each thermosyphon is equipped with a heater block and four electric cartridge heaters. Next, the test rig contains a subsystem of twelve power supplies. Each power supply is controlled independently such that a range of wattages can be delivered to the array of thermosyphons. Finally, the rig contains a Data Acquisition and Control (DAQ) system. The DAQ system monitors thermocouples placed at strategic locations on each thermosyphon and controls the power supplied to the twelve thermosyphons. Inline bimetallic thermostats installed on the heater blocks provide a means to break the electrical circuit to the heaters at the onset of the flooding limit and reinstate the electrical circuit after cooling. An artist's rendition of the Thermosyphon Array with Controlled Operation (TACO) test rig is shown in Figure 3.

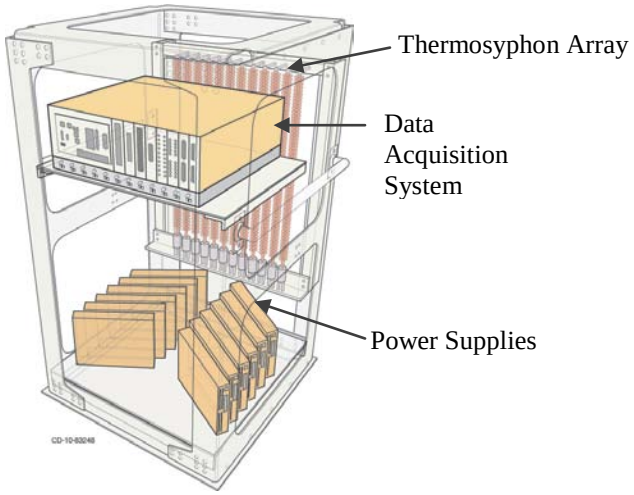

FIGURE 3. Artist's Rendition of the Thermosyphon Array with Controlled Operation (TACO) Experiment.

FUTURE PLANS

Experiments on the low-g aircraft are typically scheduled for four days of flight time. For a low-g flight, notionally, the thermosyphons in the test rig will be powered to different wattages covering a range of values over which flooding at 1/6 g is likely to occur. Hence, the range of wattages will be set by the software of the DAQ to a "coarse" range on day 1, where the increment between thermosyphons is on the order of 30 watts. Analysis of the data according to the Figure 2 should reveal a coarse estimate of the flooding limit at the time of 1/6 g exposure. For day 2, the range of wattages would be set to an "intermediate" range, where the increment between thermosyphons is on the order of 10 watts. Again, analysis according to the treatment described above should reveal an intermediate estimate of the flooding limit. By day 3, the range of wattages would be set to "fine" with the increment between thermosyphons on the order of 3 watts. Such a range should yield a fine estimate of the flooding limit. In this way, the flooding limit will be identified with ever greater resolution. Flight testing at 1/6 g will provide a means to validate the model utilized to predict flooding, thereby gaining the firsthand knowledge of how the performance of thermosyphons are affected by a reduced gravity environment.

CONCLUSION

The concept of utilizing thermosyphons at 1/6 g is introduced along with the concept of thermosyphon flooding. Tilting a thermosyphon based on the cosine function is likely a poor means of simulating thermosyphon performance at 1/6 g owing to differences in the fluid film coverage on the inside surface. Installing thermosyphons on a centrifuge and dropping the experiment in a drop tower creates a range of acceleration values along the length of any reasonably sized thermosyphon. One concept currently being considered is a low-g aircraft experiment designed to validate a mathematical model that has been worked out in detail in the literature. The model identifies the flooding limit and is often used to extrapolate performance to 1/6 g. The Thermosyphon Array with Controlled Operation Experiment is planned utilizing an array of thermosyphons. Gathering data at 1/6 g in a low-g aircraft should prove beneficial in understanding how the performance of thermosyphons is affected by a reduced gravity environment.

NOMENCLATURE

B_o = Bond number
C_{fi} = dimensionless constant
D = diameter
δ = fluid film thickness
ρ_L = density of the liquid
h_g = heat of vaporization
g = acceleration due to gravity
$\dot{m}$ = mass flow rate
R = radius
σ = surface tension
τ_i = interfacial shear force
μ_L = viscosity of the liquid
Q = energy per unit time

ACKNOWLEDGMENTS

The authors gratefully acknowledge the NASA Glenn Research Center Summer Faculty Program for their kind support of Professor Timothy A. McCollum.

REFERENCES

Ellis, D.L, "Second Generation RDU Testing Final Report, Results – Phase III," Internal Communication, May 2010.

Faghri, A., "Two-Phase Closed Thermosyphons," in *Heat Pipe Science and Technology*, Taylor & Francis Group, New York, 1995, pp. 341-440.

Katto, Y., and Watanabe, K., 1992, "An Analytic Study on the Critical Heat Flux of Countercurrent Boiling in a Vertical Tube with a Closed Bottom," *International Journal of Heat and Mass Transfer*, Vol. 35, No. 11, 3021-3028 (1992).

Shatto, D.P, Besly, J.A., Peterson, G.P., "A visualization study of flooding and entrainment in a closed two-phase thermosyphon," *AIAA, Thermophysics Conference*, New Orleans, LA, 1996.